Electronic Supplementary Material (ESI) for New Journal of Chemistry.

Supplementary Material

-"Manganese(II) Thiophosphate ($MnPS_3$) Intercalates with Lanthanide (Pr^{III} and Nd^{III}) Complexes: Optical and Magnetic Properties"

Pablo Fuentealba, Jeannette Morales, Nathalie Audebrand, Claudio José Magon, Hellmut Eckert, Jorge Manzur, Evgenia Spodine

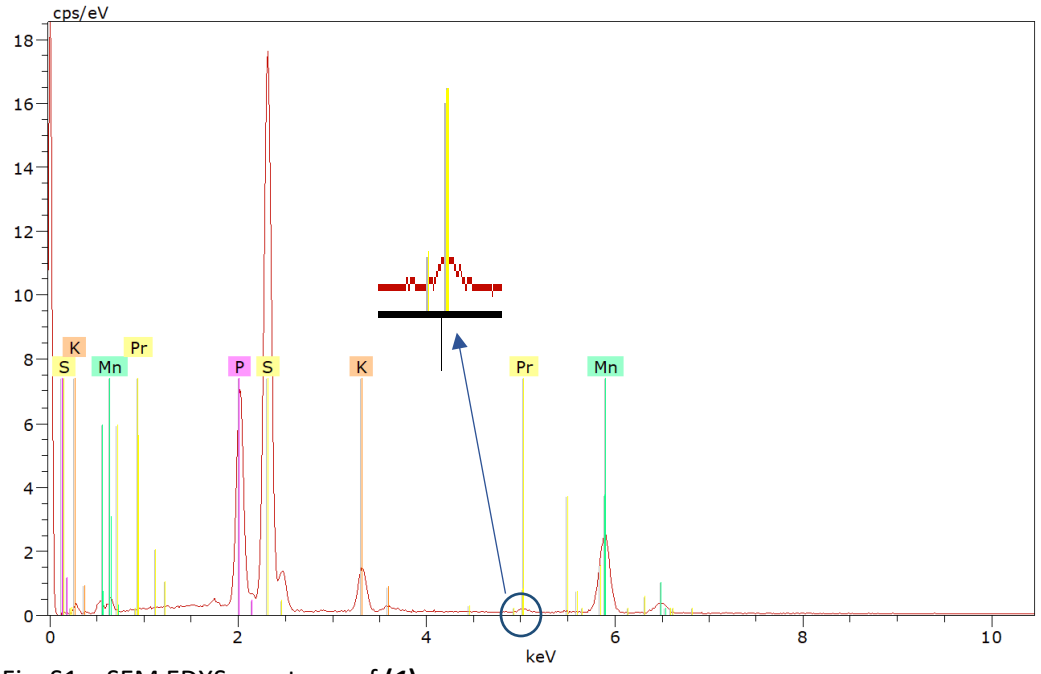

Fig. S1a. SEM EDXS spectrum of ***(1)*.**

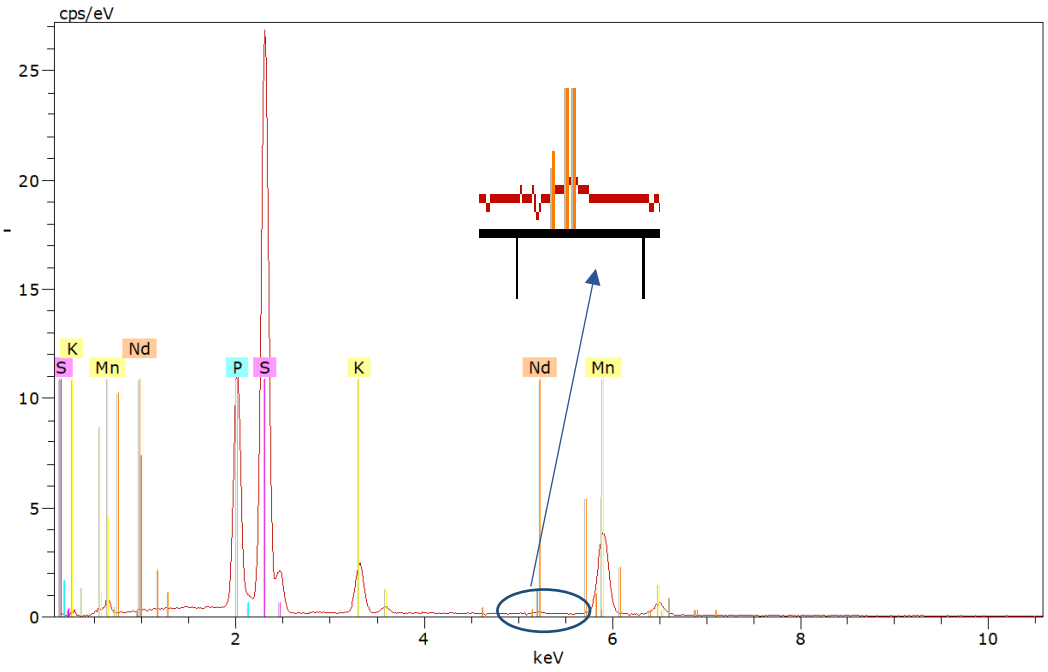

Fig. S1b. SEM EDXS spectrum of ***(2)*.**

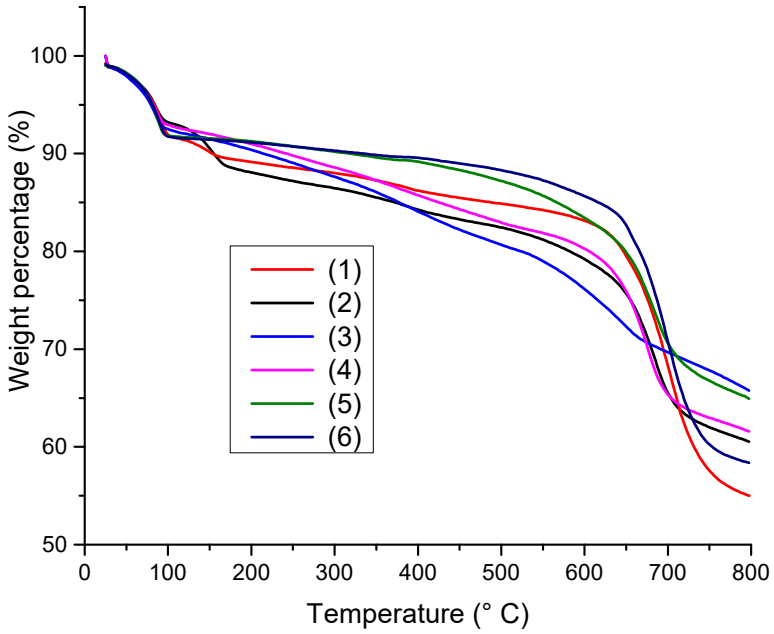

Fig. S2. TGA curves of the intercalation compounds ***1-6***.

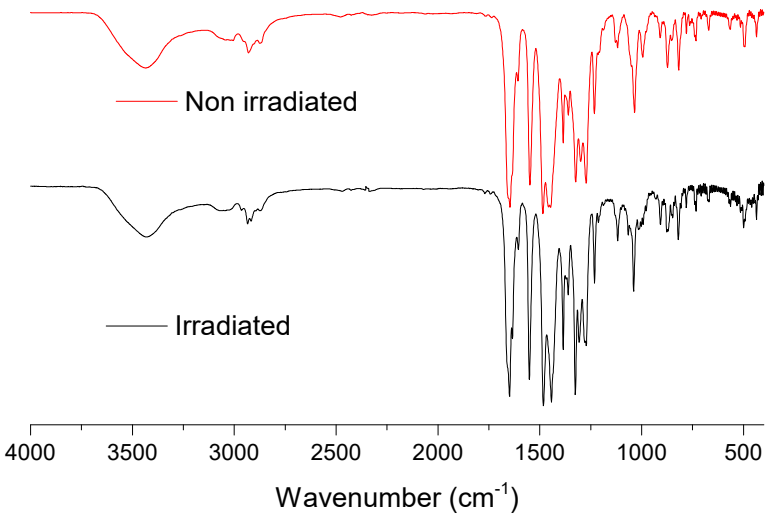

Fig.S3a. FTIR spectra of the $[PrL^2H_2(NO_3)_3]$ complex before and after irradiation (modification of the spectra was not observed for the irradiated complexes).

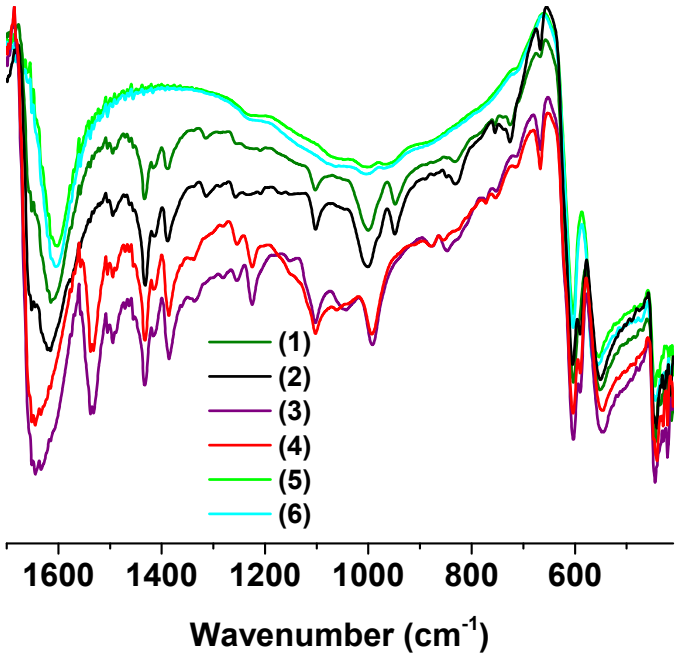

Fig S3b. FTIR spectra of the intercalation compounds ***1-6***.

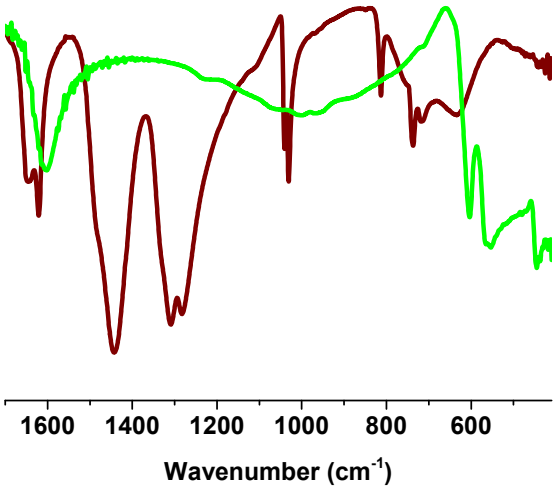

Fig S3c. FTIR spectra of $Pr(NO_3)_3 \cdot xH_2O$ salt (brown) and intercalate **(5)** (light green), indicating the absence of the nitrate band at

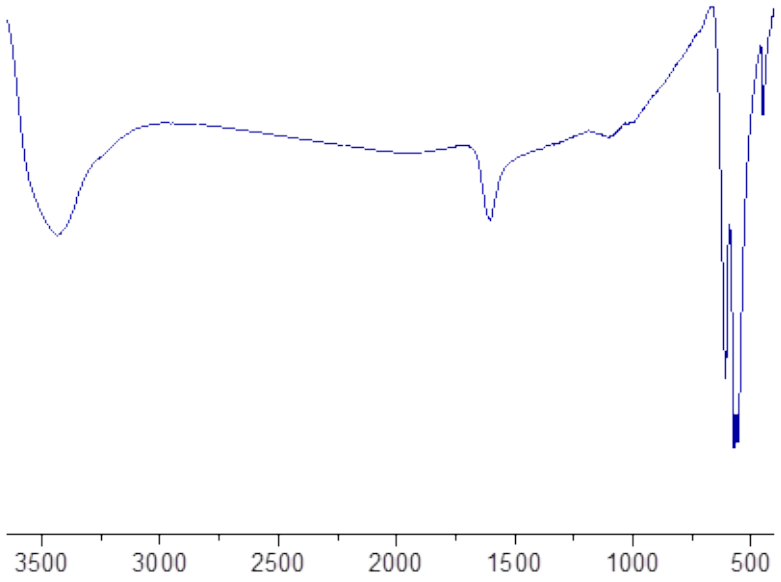

Fig S3d. FTIR Spectrum of $K_{0.4}Mn_{0.8}PS_3 \cdot H_2O$.

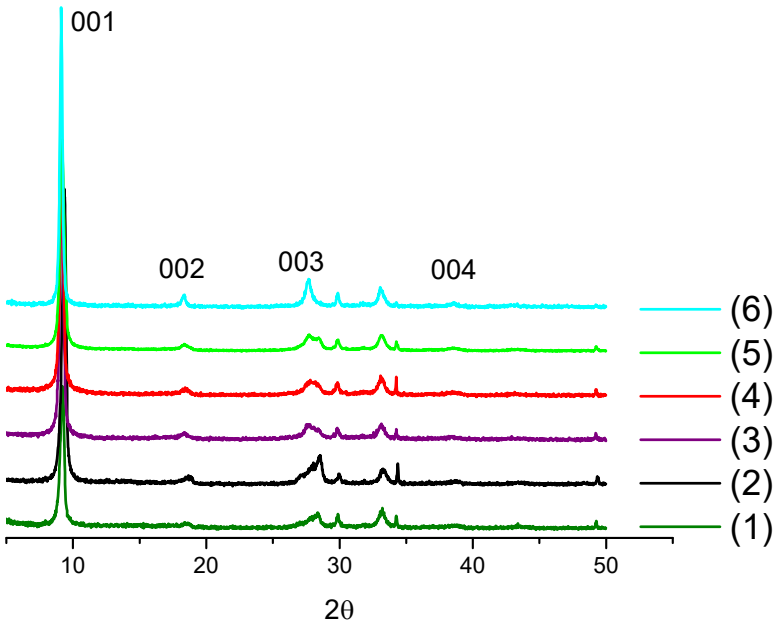

Fig S4. Powder X-ray diffractograms of the obtained intercalates. Reflections with Miller indexes 00*l* have been highlighted.

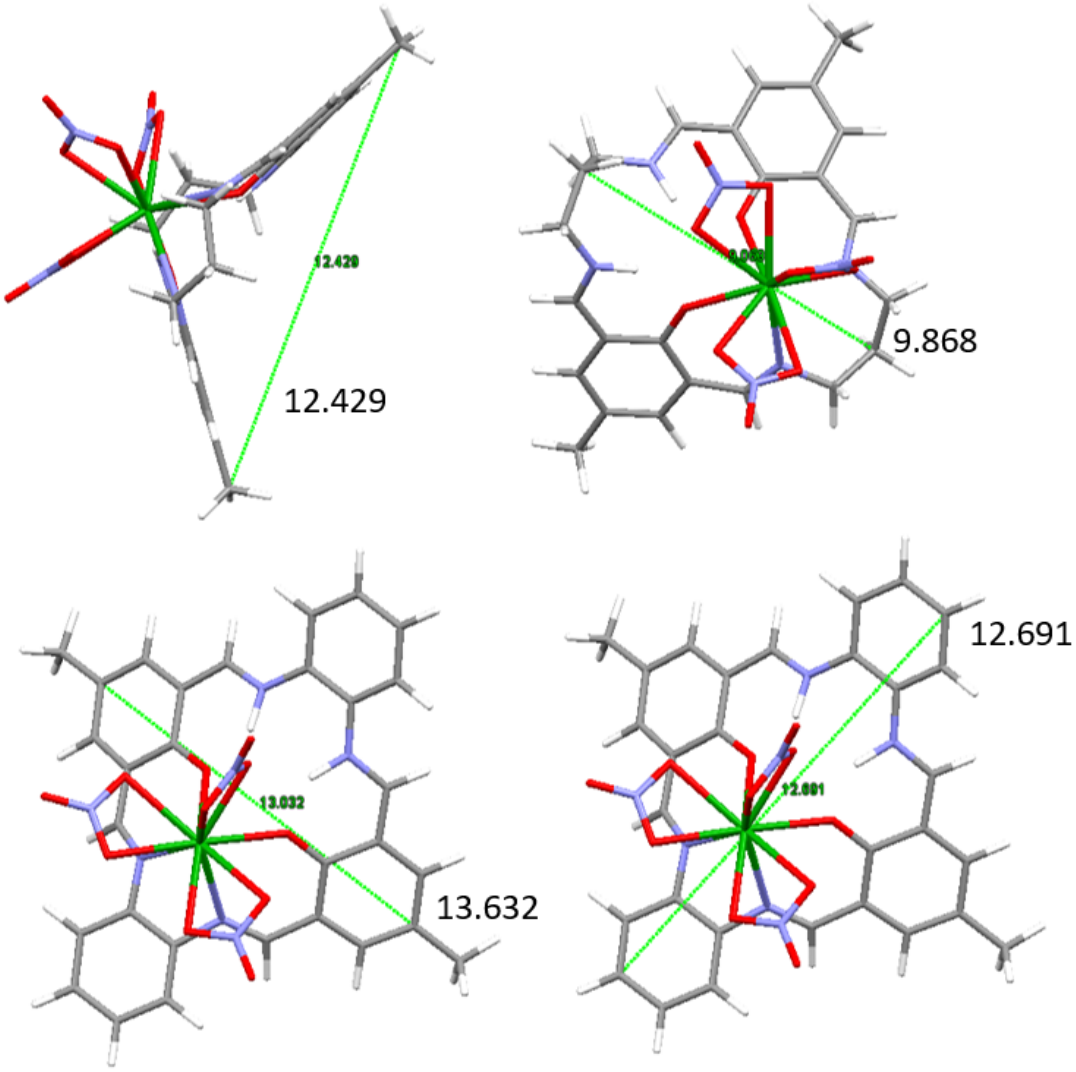

Figure S5. Dimensions of the macrocyclic complexes before the intercalation process.

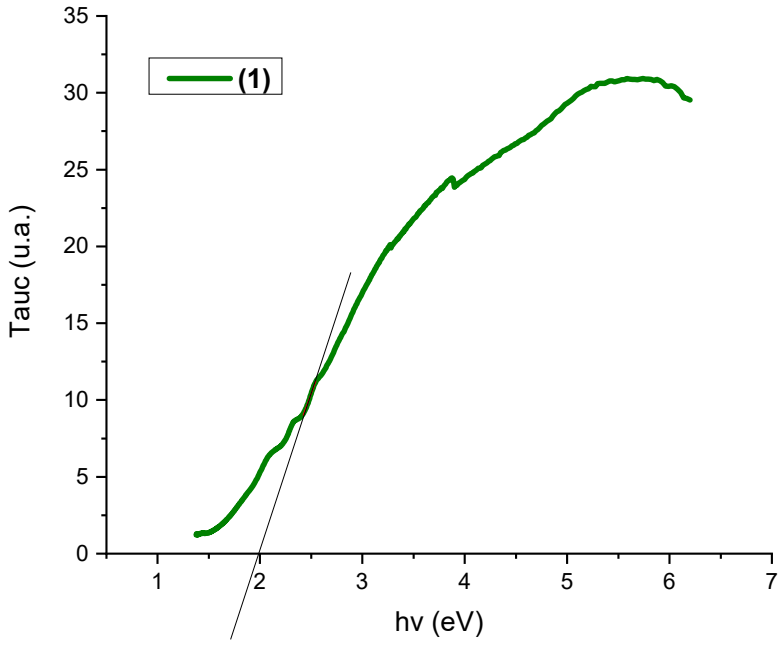

Figure S6a. Tauc plot for composite **(1)**.

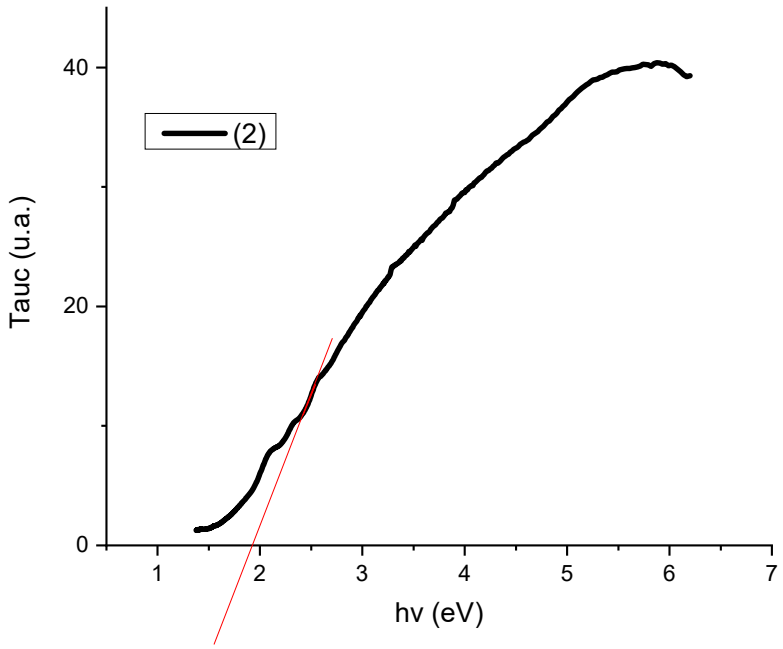

Figure S6b. Tauc plot for composite **(2)**.

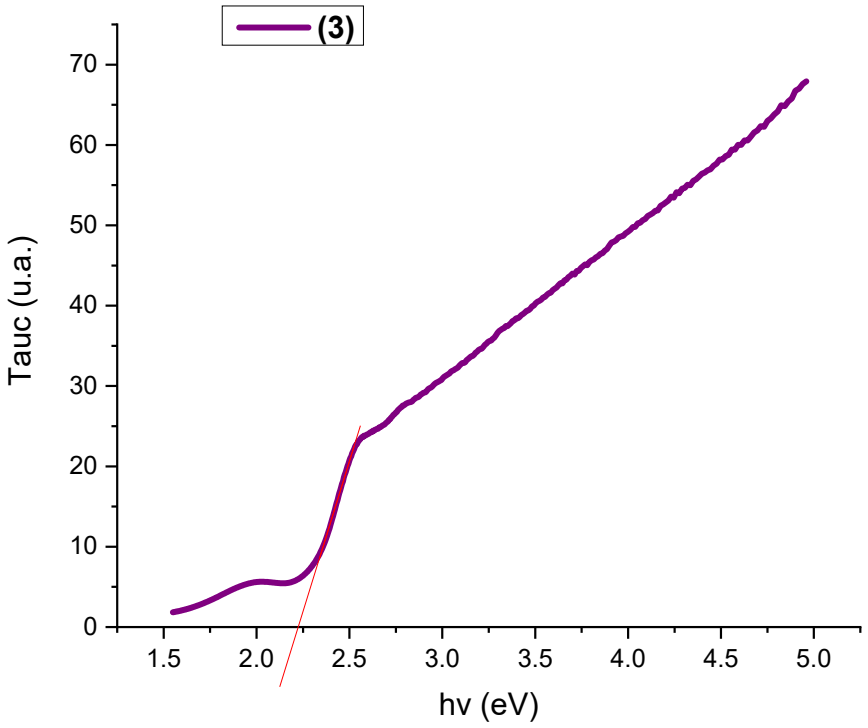

Figure S6c. Tauc plot for composite **(3)**.

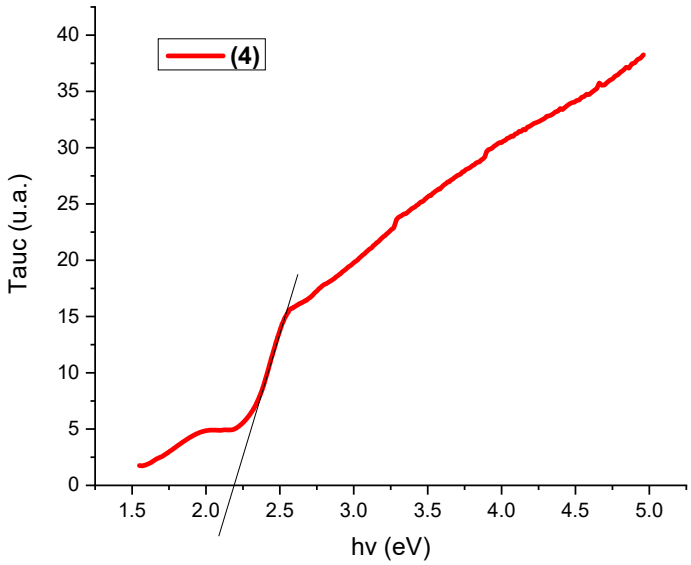

Figure S6d. Tauc plot for composite **(4)**.

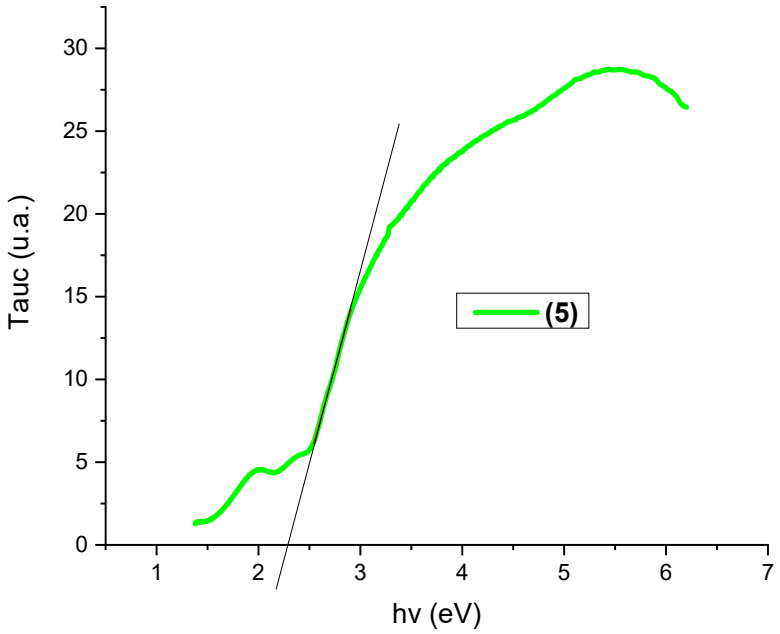

Figure S6e. Tauc plot for composite **(5)**.

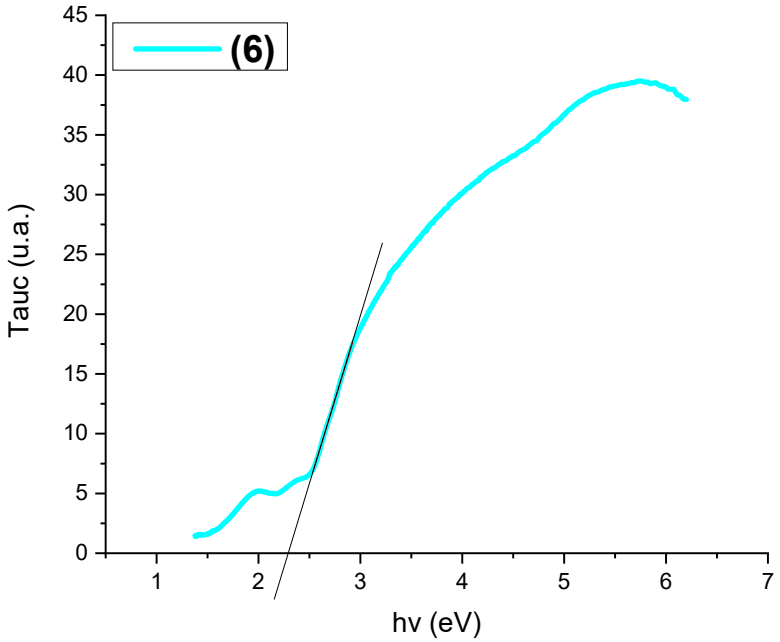

Figure S6f. Tauc plot for composite **(6)**.

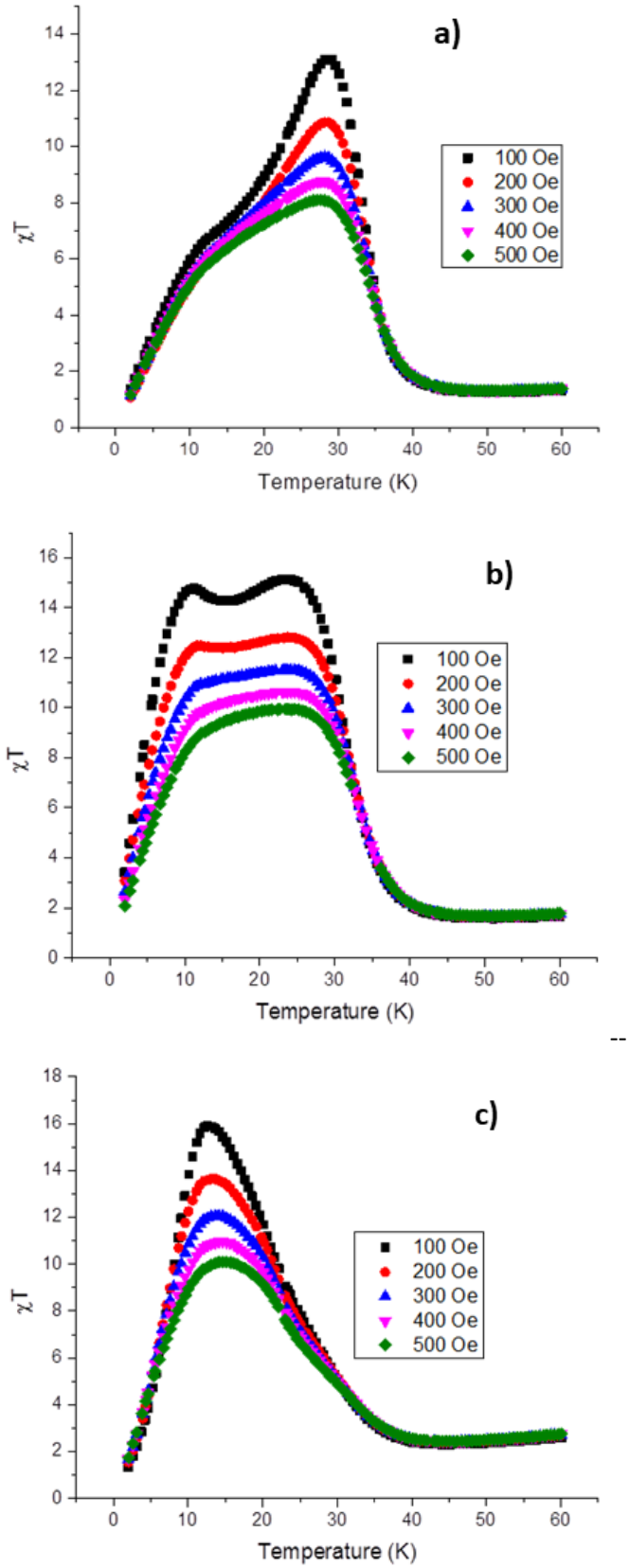

Fig. S7: Temperature dependence of the product χT measured for the intercalates derived from Nd(III) species at different magnetic field strengths.

a) $[NdL^1H_2]_{0.01}K_{0.37}Mn_{0.8}PS_3{\cdot}0.9H_2O$ (***2***); b) $[NdL^2H_2]_{0.05}K_{0.25}Mn_{0.8}PS_3{\cdot}0.9H_2O$ (***4***);
c) $[Nd]_{0.03}K_{0.31}Mn_{0.8}PS_3{\cdot}0.8H_2O$ (***6***)

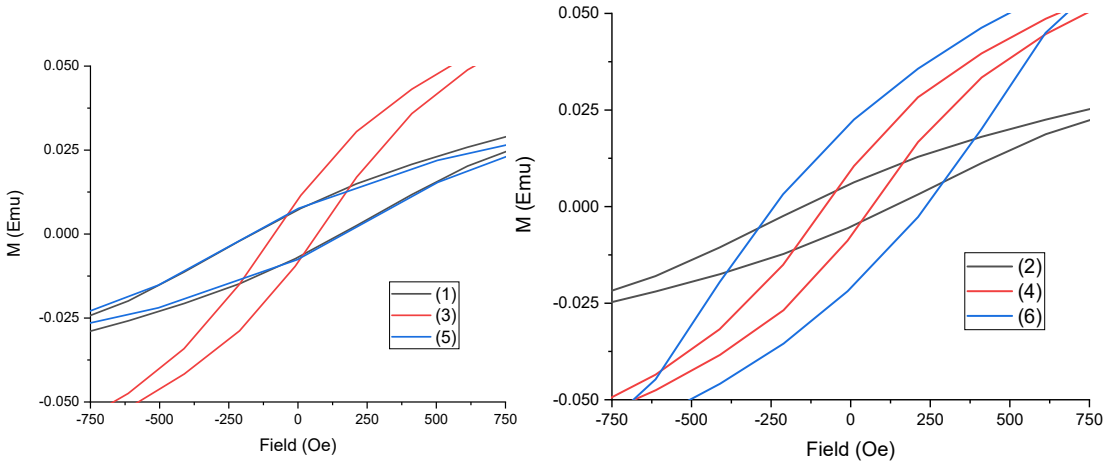

Figure S8. Hysteresis loops for all intercalates; left, for praseodymium intercalates and right, for the neodymium ones.

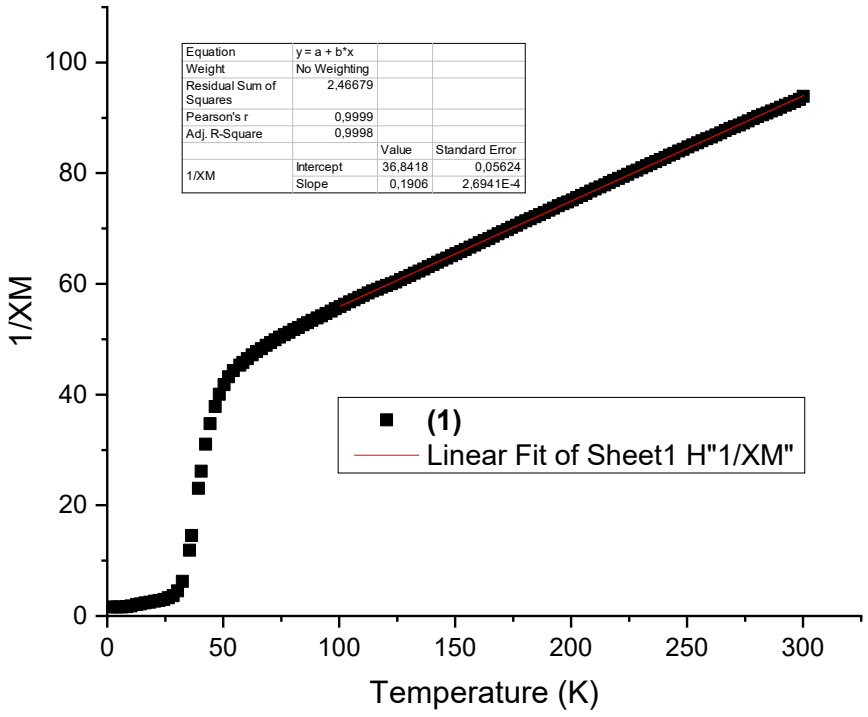

Figure S9a. Curie-Weiss fitting for **(1)**

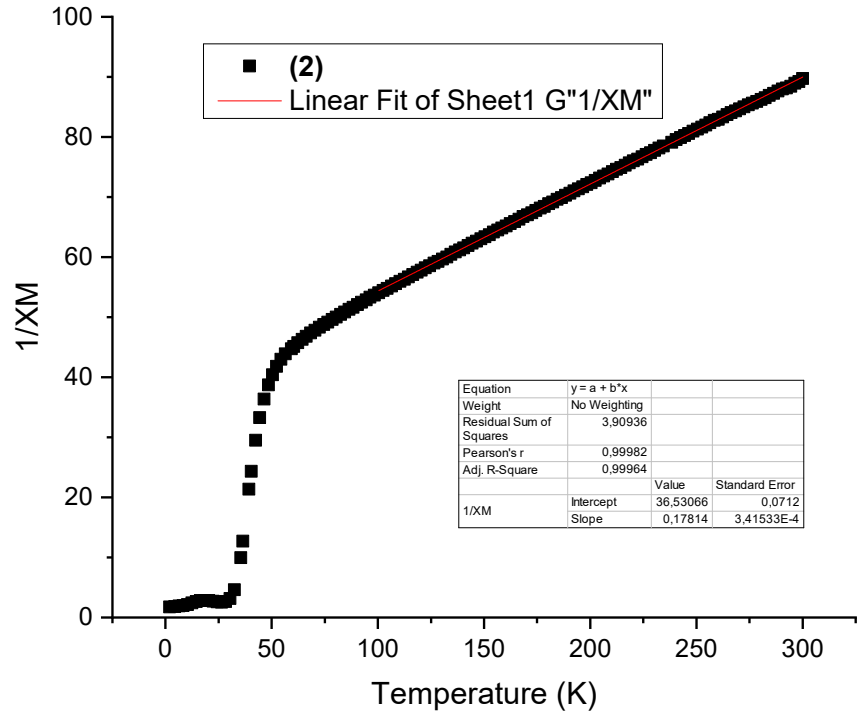

Figure S9b. Curie-Weiss fitting for **(2)**

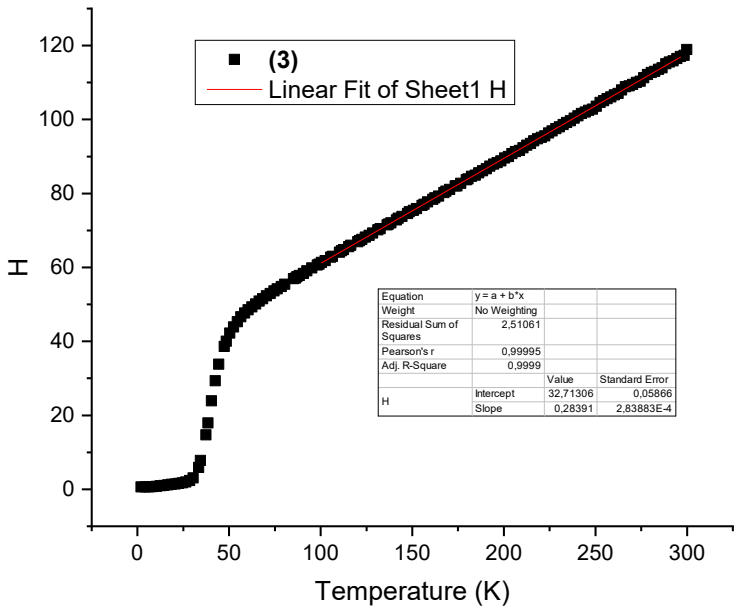

Figure S9c. Curie-Weiss fitting for **(3)**

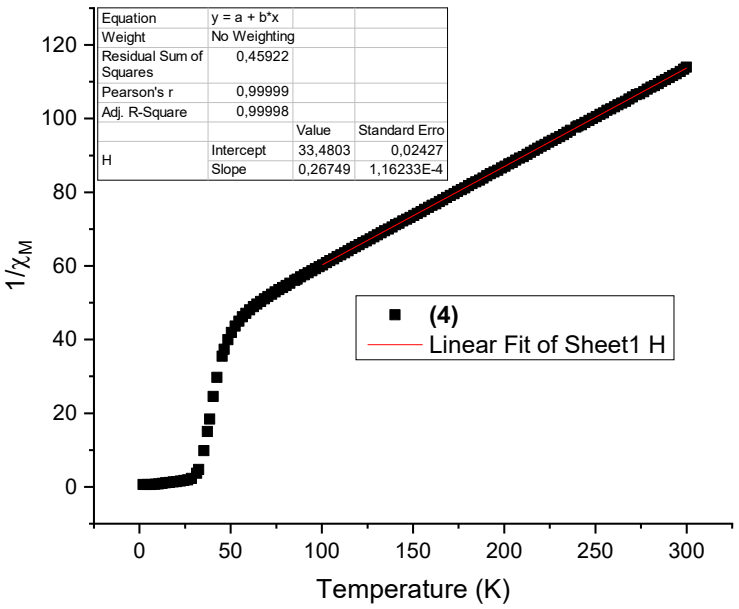

Figure S9d. Curie-Weiss fitting for **(4)**

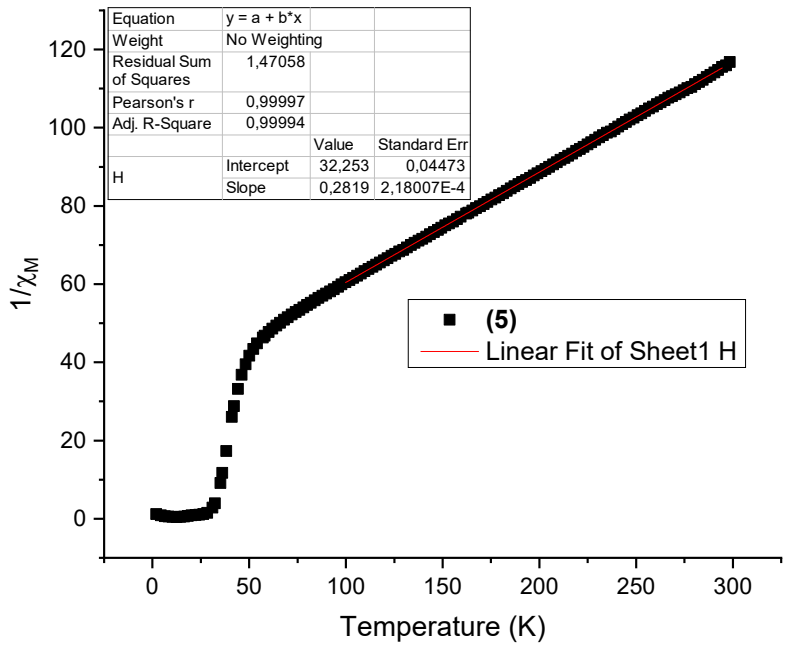

Figure S9e. Curie-Weiss fitting for **(5)**

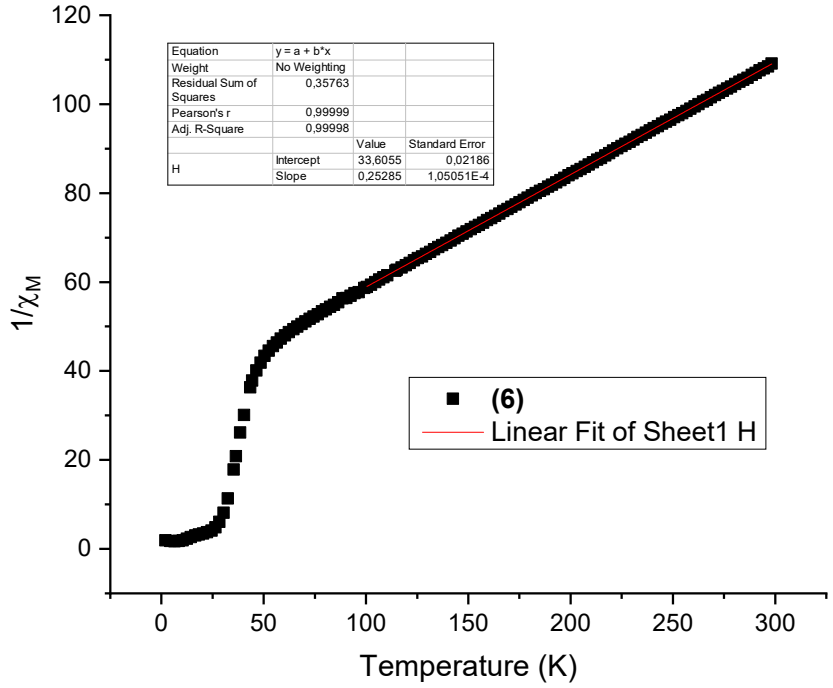

Figure S9f. Curie-Weiss fitting for **(6)**

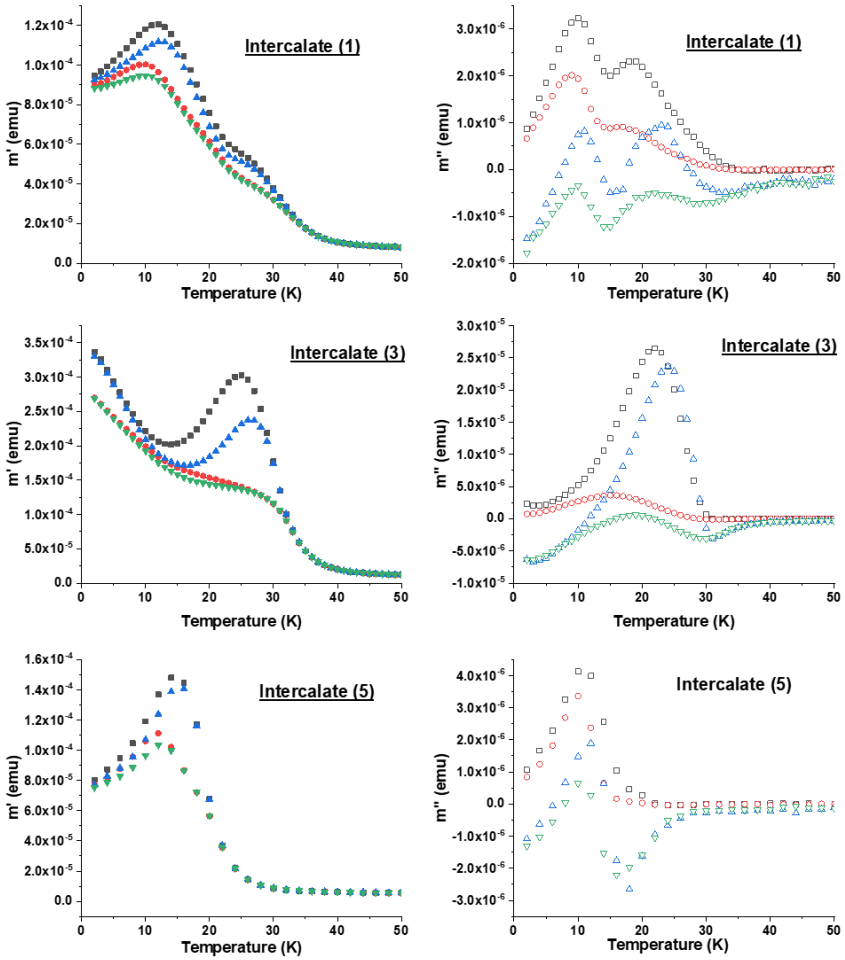

Fig. S9a. AC magnetic susceptibility for the praseodymium(III) intercalates ***1***,***3***, and ***5***. Solid symbols for m' and open symbols for m''. Drive field 3Oe. Black squares: 0 Oe-10 Hz. Red circles: 100 Oe-10 Hz. Blue up-triangles: 0 Oe-1.000 Hz. Green down-triangles: 100 Oe-1.000 Hz.

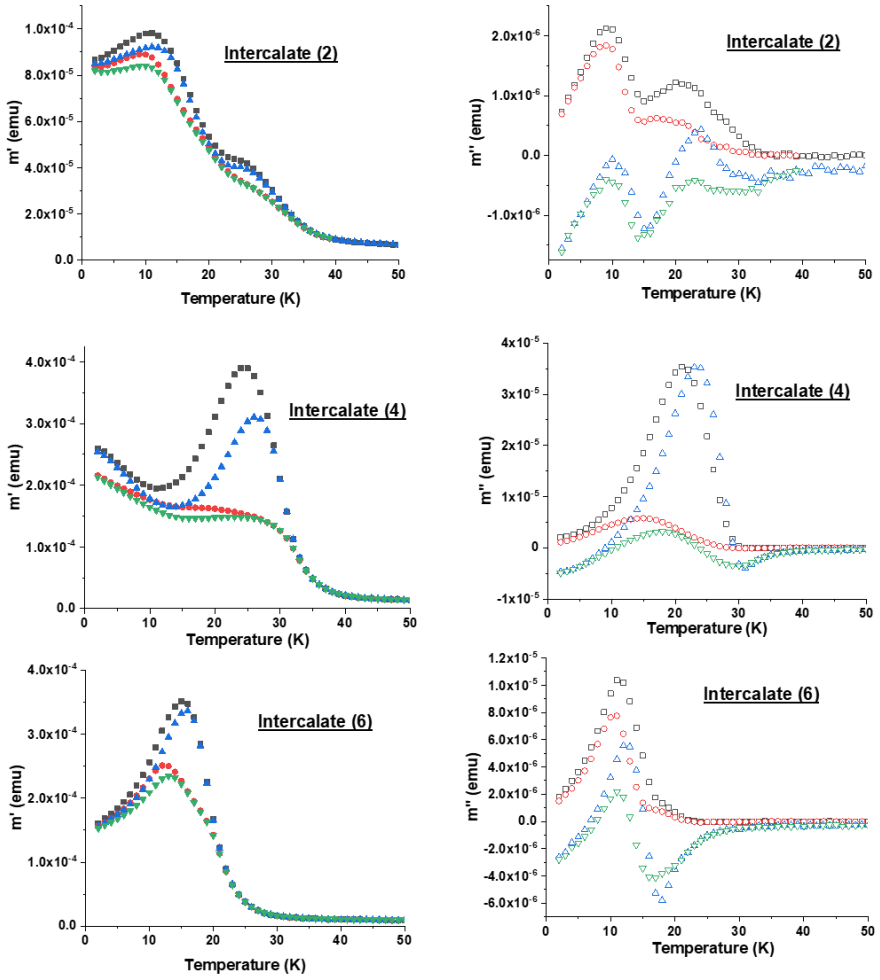

Fig. S9b. AC magnetic susceptibility for the neodymium(III) intercalates ***2***,***4***, and ***6***. Solid symbols for m' and open symbols for m''. Drive field 3Oe. Black squares: 0 Oe-10 Hz. Red circles: 100 Oe-10 Hz. Blue up-triangles: 0 Oe-1.000 Hz. Green down-triangles: 100 Oe-1.000 Hz.

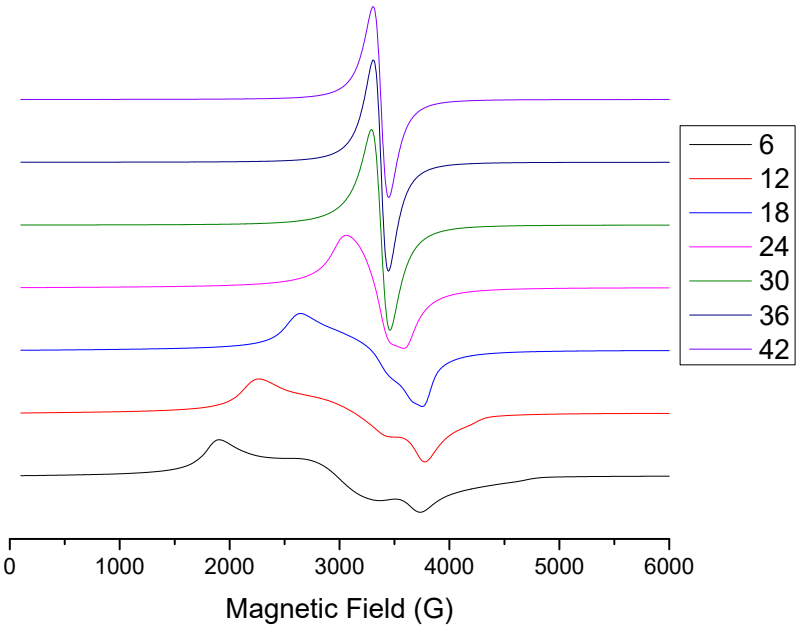

Fig. S10a: Temperature dependent EPR spectra of the intercalate **(6)**

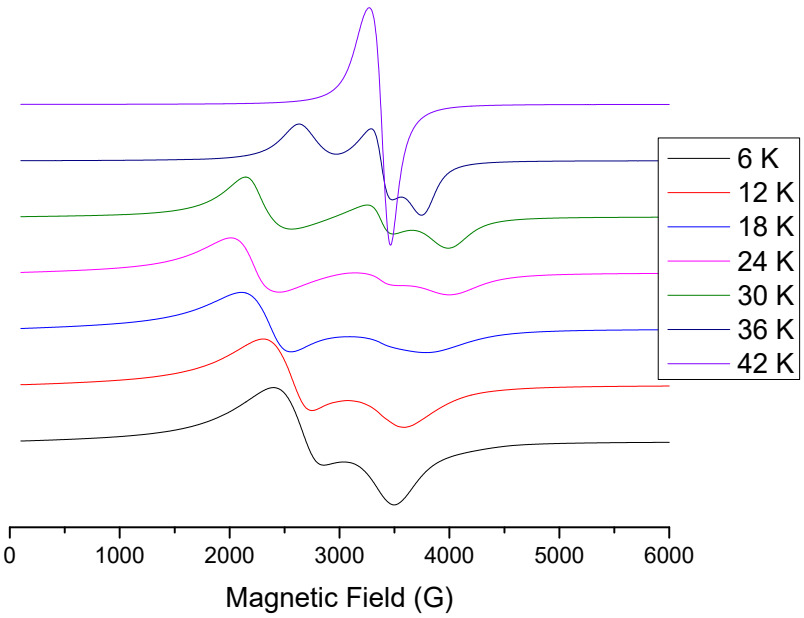

Fig. S10b: Temperature dependent EPR spectra of the intercalate **(2)**

Table S1: Unit-cell parameters refined by pattern-matching for the powder X-ray diffraction patterns. A monoclinic *C*2/*m* unit cell was used.

(1) $[PrL^1H_2]_{0.01}K_{0.37}Mn_{0.8}PS_3{\cdot}0.9H_2O$
(2) $[NdL^1H_2]_{0.01}K_{0.37}Mn_{0.8}PS_3{\cdot}0.9H_2O$
(3) $[PrL^2H_2]_{0.05}K_{0.25}Mn_{0.8}PS_3{\cdot}0.9H_2O$
(4) $[NdL^2H_2]_{0.05}K_{0.25}Mn_{0.8}PS_3{\cdot}0.9H_2O$
(5) $[Pr]_{0.01}K_{0.37}Mn_{0.8}PS_3{\cdot}0.8H_2O$
(6) $[Nd]_{0.01}K_{0.37}Mn_{0.8}PS_3{\cdot}0.8H_2O$

	(*1*)	**(*2*)**	**(*3*)**	**(*4*)**	**(*5*)**	**(*6*)**
a(Å)	6.106(1)	6.0821(8)	6.095(3)	6.088(2)	6.104(5)	6.094(4)
b(Å)	10.560(2)	10.552(1)	10.556(7)	10.544(4)	10.666(8)	10.687(8)
c (Å)	9.5728(6)	9.6057(9)	9.597(5)	9.589(8)	9.533(3)	9.478(4)
β (°)	101.72(1)	101.69(8)	101.70(6)	101.90(3)	100.75(5)	101.06(3)
d (Å)	9.70	9.70	9.70	9.70	9.70	9.70

	$MnPS_3$[1]	$K_{0.4}Mn_{0.8}PS_3$[2]	$K_{0.32}[Zn_2L]_{0.04}Mn_{0.8}PS_3$[2]	$K_{0.24}[Cu_2L]_{0.08}Mn_{0.8}PS_3$[2]
a(Å)	6.077	6.11	6.095	6.092
b(Å)	10.524	10.59	10.571	10.509
c (Å)	6.796	9.64	10.415	10.417
β (°)	107.35	102.20	102.56	102.71
d (Å)	6.50	9.40	10	10

d interlamellar distance. *

References:

(1) Ouvrard, G.; Brec, R.; Rouxel, J. Structural Determination of Some MPS_3 Layered Phases (M = Mn, Fe, Co, Ni and Cd). *Mater. Res. Bull.* **1985**, *20* (10), 1181–1189 DOI: 10.1016/0025-5408(85)90092-3.

(2) Fuentealba, P.; Paredes-Garcia, V.; Venegas-Yazigi, D.; Silva, I. D. A.; Magon, C. J.; Costa de Santana, R.; Audebrand, N.; Manzur, J.; Spodine, E. Magnetic Properties of Composites Based on the Intercalation of Zn II and Cu II Bimetallic Macrocyclic Complexes in the MnPS 3 Phase. *RSC Adv.* **2017**, *7* (53), 33305–33313 DOI: 10.1039/C7RA05089E.